



# SYNTHESIS AND CHARACTERIZATION OF NANOCOMPOSITES HAVING CATALYTIC ACTIVITIES USING MICROWAVE TECHNIQUES

M.S. Al-Amoudi<sup>[a]\*</sup>, M.S. Salman<sup>[a]</sup>, A.S. Megahed<sup>[a]</sup> and M.S. Refat<sup>[a]</sup>

**Keywords:** 4-Hydroxybenzoic acid; Cobalt(II) ions; X-ray powder diffraction; Spectroscopic data; Thermal analysis; Nanocomposites; Biological evaluation;

A new cobalt(II) 4-hydroxybenzoate,  $[\text{Co}_2(\text{C}_7\text{H}_5\text{O}_3)_2(\text{NO}_3)_2(\text{H}_2\text{O})_4]2\text{H}_2\text{O}$  was synthesized as binuclear complex and characterized by elemental analyses (CHN), spectroscopic (infrared, electronic, x-ray powder diffraction, scanning electron microscopy SEM,) studies, magnetic susceptibility measurements and thermal analysis. This complex is a new type of 4-hydroxybenzoate bridged metal complex in which the carboxylate ligand is *p*-hydroxybenzoic acid. Bridging co-ordination modes for the carboxylates were indicated by the presence of ( $\nu_{\text{asym}}-\nu_{\text{sym}}$ ) vibrations in the infrared spectra nearly the same as observed for ionic compounds. The magnetic moment value of cobalt(II) 4-hydroxybenzoate determined in at 300 K is 4.45 BM which refer to octahedral geometry. Thermo gravimetric analysis (TGA) of the hydrated water molecules shows that the first degradation step is associated with the release of water molecules followed by the decomposition of the 4-hydroxybenzoate, nitrate and coordinated water molecules. According to Horowitz-Metzger (HM) and Coats-Redfern methods, the kinetic parameters for the non-isothermal degradation of this complex were calculated using thermogravimetric data.

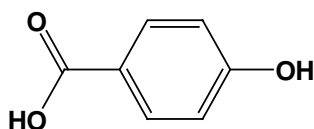
\* Corresponding Authors

e-mail: dr\_alamoudi@yahoo.com

[a] Department of Chemistry, Faculty of Science, Taif University, 888 Taif, Kingdom Saudi Arabia

## Introduction

4-Hydroxybenzoic acid is a mono-hydroxybenzoic acid, a phenolic derivative of benzoic acid. It is a white crystalline solid, slightly soluble in water and chloroform but more soluble in polar organic solvents such as alcohols and acetone. 4-Hydroxybenzoic acid is primarily known as the basis for the preparation of its esters, known as parabens, which are used as preservatives in cosmetics and some ophthalmic solutions. It is isomeric with 2-hydroxybenzoic acid, known as salicylic acid, a precursor to aspirin. 4-Hydroxybenzoic acid can be found naturally in *Cocos nucifera*.<sup>1</sup> It is one of the main catechins metabolites found in human beings after consumption of green tea infusions.<sup>2</sup>

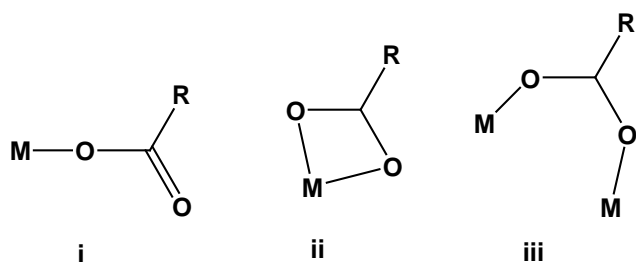


**Formula 1:** Structure of 4-hydroxybenzoic acid

The chemistry of metal carboxylates continues to be an area of intense research in view of its diverse applications, ranging from the relevance of metal carboxylate complexes as model systems for the metal-active sites in bioinorganic chemistry<sup>3,4</sup> to their use as novel materials in material science. Metal oxides can be readily prepared from metal carboxylate by thermal decomposition methods.<sup>5</sup> Metal carboxylates exhibit fascinating structural features. The

structure diversity of metal carboxylate complexes can be attributed to the versatile ligational behaviour of the carboxylate group which can function like a bidentate ligand binding with single metal atom or alternatively as a bridging bidentate ligand coordinating two metal atoms or as a monodentate ligand.<sup>6-8</sup> The metal carboxylates have high affinity to chelate with the transition metal ions, hence are attracting attention due to potential applications in areas viz. biology, catalysis, thermal, electrical, optical, magnetic, etc.<sup>9-14</sup> The structural diversity encountered in metal-carboxylate complexes can be attributed to the versatile ligational behavior of the carboxylate group which can function like a bidentate ligand binding to a single metal or alternatively as a bridging bidentate ligand coordinating to two metals or as a monodentate ligand<sup>15,16</sup> The carboxylate group is able to coordinate to metal ions by different modes (Scheme 1).<sup>17</sup>

- (i) When the carboxylate group coordinates the metal ion in a monodentate manner, the difference between the wavenumbers of the asymmetric and symmetric carboxylate stretching bands,  $\Delta\nu = \nu_{\text{as}}\text{COO}^- - \nu_{\text{s}}\text{COO}^-$ , is larger than that observed for ionic compounds.
- (ii) When the ligand chelates,  $\Delta\nu$  is considerably smaller than that for ionic compounds, while on the asymmetric bidentate coordination, the values is in the range characteristic of monodentate coordination.<sup>18</sup>
- (iii) The characteristic wavenumber difference,  $\Delta\nu$ , is larger than that for chelated ions and nearly the same as observed for ionic compounds. Based on the above results, it was possible to distinguish the coordination mode of the  $-\text{COO}^-$  group.



**Scheme 1.** Possible coordination modes of the carboxylate group

Cobalt(II) of 4-hydroxybenzoic acid complex is a little known. Ammonium ( $\text{NH}_4^+$ ) and sodium 4-hydroxybenzoate were prepared as solid compounds soluble in water. The binuclear cobalt(II) complex with p-hydroxybenzoic acid has not been studied before. The main purpose of the present work has been the study of some physicochemical properties, thermal degradation and the ability of binuclear cobalt(II) p-hydroxybenzoic acid to act as a bio-mimetic heterogeneous catalyst for selective oxidation of various alcohols with  $\text{H}_2\text{O}_2$ . The catalytic behavior of cobalt(II) complex can be discussed upon the micro-porous structure which constructed by intermolecular bridging of Co-OO-Co species. In order to obtain a wide insight into cobalt(II) hydroxybenzoic acid complex properties, the FT-IR, UV-vis, magnetic measurements, SEM, XRD analysis and (TG/TGA) studies were carried out and the results are presented in connection with the kinetic parameters for the non-isothermal degradation of the two maximum DTG peaks by using Horowitz Metzger (HM) and Coats-Redfern (CR) methods. Microwave-assisted synthesis is a branch of green chemistry. The application of microwave-assisted synthesis in organic, organometallic and coordination chemistry continues to develop at an astonishing pace. Microwave irradiated reactions under solvent free or minimum solvent conditions are attractive to reduced pollution, cost effectiveness and provide high yields together with simple processing and handling.<sup>19-23</sup>

## Experimental

### Chemicals and reagents

All chemicals and reagents used in present study were of analytical grade. 4-Hydroxybenzoic acid and cobalt (II) nitrate were received from Aldrich and Fluka chemical companies.

### Microwave method for the synthesis of cobalt(II) complex

The 4-hydroxybenzoic acid ligand and the cobalt(II) nitrate hexahydrate were mixed in 1:2 (metal:ligand) ratio at pH= 8 with ammonia solution. The reaction mixture was then irradiated by the microwave oven with 10-15 mL of dry ethanol as solvent. The reaction was completed in a short time (5 min) with higher yields. The resulting product was then washed with ethanol and ether and finally dried under reduced pressure over anhydrous  $\text{CaCl}_2$  in a desiccator. The progress of the reaction and purity of the product was monitored by TLC using silica gel G (yield: 85%).

### Physical measurements and analytical estimations

The elemental analyses of carbon, hydrogen and nitrogen contents were performed using a Perkin Elmer CHN 2400, while content of cobalt was determined from TG curves and by calcinating the prepared complex to most stable oxide ( $\text{Co}_2\text{O}_3$ ) at 800 °C. The content of crystallization water was calculated from TG curves and by heating the complex at appropriate temperature. The molar conductivity of freshly prepared  $1.0 \times 10^{-3}$  mol/cm<sup>3</sup> dimethylsulfoxide (DMSO) solution was measured for the dissolved cobalt(II) 4-hydroxybenzoic acid complex using Jenway 4010 conductivity meter. The electronic absorption spectra of cobalt(II) complex was recorded in DMSO solvent within 900-200 nm range using a UV2 Unicam UV/Vis Spectrophotometer fitted with a quartz cell of 1.0 cm path length in Mansoura University. The infrared spectra with KBr discs were recorded on a Bruker FT-IR Spectrophotometer (4000–400  $\text{cm}^{-1}$ ). Solid reflectance spectra were measured on UV-3101 PC, Shimadzu, UV-Vis. NIR Scanning Spectrophotometer. Magnetic data were calculated using Magnetic Susceptibility Balance, Sherwood Scientific, Cambridge Science Park Cambridge, England, at Temp 25°C in Cairo University. The thermal studies TG/DTG-50H were carried out on a Shimadzu thermogravimetric analyzer under static air till 800 °C. Scanning electron microscopy (SEM) images were taken in Quanta FEG 250 equipment. The X-ray diffraction patterns for the studies cobalt(II) complex was recorded on X 'Pert PRO PANanalytical X-ray powder diffraction, target copper with secondary monochromate.

### Antibacterial and antifungal activities

Antimicrobial activity of the tested samples was determined using a modified Kirby-Bauer disc diffusion method.<sup>24</sup> Briefly, 100  $\mu\text{l}$  of the best bacteria/fungi were grown in 10 mL of fresh media until they reached a count of approximately 10<sup>8</sup> cells/mL for bacteria or 10<sup>5</sup> cells/mL for fungi.<sup>25</sup> 100  $\mu\text{l}$  of microbial suspension was spread onto agar plates corresponding to the broth in which they were maintained. Isolated colonies of each organism that might be playing a pathogenic role should be selected from primary agar plates and tested for susceptibility by disc diffusion method.<sup>26,27</sup> Of the many media available, National Committee for Clinical Laboratory Standards (NCCLS) recommends Mueller-Hinton agar due to: it results in good batch-to-batch reproducibility. Disc diffusion method for filamentous fungi tested by using approved standard method (M38-A) developed by the NCCLS<sup>28</sup> for evaluating the susceptibility of filamentous fungi to antifungal agents. Disc diffusion method for yeast developed standard method (M44-P) by the NCCLS.<sup>29</sup> Plates inoculated with filamentous fungi as *Aspergillus Flavus* at 25 °C for 48 hours; Gram (+) bacteria as *Staphylococcus Aureus*, *Bacillus subtilis*; Gram (-) bacteria as *Escherichia Coli*, *Pseudomonas aeruginosa* they were incubated at 35-37 °C for 24-48 hours and yeast as *Candida Albicans* incubated at 30 °C for 24-48 hours and, then the diameters of the inhabitation zones were measured in millimetres.<sup>24</sup> Standard discs of Tetracycline (Antibacterial agent), Amphotericin B (Antifungal agent) served as positive controls for antimicrobial activity but filter disc impregnated with 10  $\mu\text{l}$

of solvent (distilled water, DMSO) were used as a negative control. The agar used is Mueller-Hinton agar that is rigorously tested for composition and pH. Further the depth of the agar in the plate is a factor to be considered in the disc diffusion method. This method is well documented and standard zones of inhibition have been determined for susceptible values. Blank paper disks (Schleicher & Schuell, Spain) with a diameter of 8.0 mm were impregnated 10  $\mu\text{l}$  of tested concentration of the stock solutions. When a filter paper disc impregnated with a tested chemical is placed on agar the chemical will diffuse from the disc into the agar. This diffusion will place the chemical in the agar only around the disc. The solubility of the chemical and its molecular size will determine the size of the area of chemical infiltration around the disc. If an organism is placed on the agar it will not grow in the area around the disc if it is susceptible to the chemical. This area of no growth around the disc is known as a "Zone of inhibition" or "Clear zone". For the disc diffusion, the zone diameters were measured with slipping calipers of the National Clinical Laboratory Standards.<sup>26</sup> Agar-based methods such as Etest disk diffusion can be good alternatives because they are simpler and faster than broth methods.<sup>30,31</sup>

## Results and discussions

### Analytical data and conductivity measurements

The molecular weights, molecular formula and percentage of each carbon, hydrogen and nitrogen contents of cobalt(II) 4-hydroxybenzoate complex was listed in Table 1. The elemental analysis technique support the stoichiometry between 4-hydroxybenzoic acid and cobalt(II) nitrate salt is 1:1. The microwave-assisted synthesis technique lead to complete the chemical reaction in a short time with higher yields compared to the usual method. In the microwave method homogeneity of reaction mixture was increased by the rotating of reaction platform tray. The cobalt(II) p-hydroxybenzoate complex has a pink color, solid and stable with hygroscopic nature at room temperature. Conductivity meter type Jenway 4010 was used to measure conductivities of cobalt(II) hydroxybenzoate complex of p-hydroxybenzoic acid ligand in DMSO with  $1.0 \times 10^{-3} \text{ mol dm}^{-3}$  concentration. The conductivity of the free ligand was also measured at a similar condition in order to make comparison between the free ligand with its respective cobalt(II) complex. The conductance value of this complex is  $50 \Omega^{-1} \text{ cm}^{-1} \text{ mol}^{-1}$ . The conductance value indicates that this complex has slightly electrolytic in nature. Slightly electrolytic complex assigned to the presence of nitrate groups inside chelation.<sup>17</sup>

### Infrared spectra

The infrared spectral data of sodium p-hydroxybenzoate and cobalt(II) complex (Fig. 1) were characterized and presented in Table 2. The band at  $1694 \text{ cm}^{-1}$  originating from  $-\text{COOH}$  stretching vibration, in the spectrum of the p-hydroxybenzoic acid, is replaced in the spectra of cobalt(II) complex, by two bands at  $1607 \text{ cm}^{-1}$  and  $1385 \text{ cm}^{-1}$ , which can be ascribed to the asymmetric and symmetric vibrations of  $-\text{COO}-$  groups, respectively.<sup>32</sup> The bands attributed to asymmetric and symmetric C-H stretching modes of the aromatic rings are observed at  $3181 \text{ cm}^{-1}$ . The bands with

the maxima at  $3602$  and  $3381 \text{ cm}^{-1}$  in the spectrum of 4-hydroxybenzoate of Co(II) are characteristic for  $\nu(\text{O-H})$  vibrations<sup>32,33</sup> of water molecules and  $-\text{OH}$  hydroxyl benzoic acid free of chelation. The bands of  $\nu(\text{C}=\text{C})$  ring vibrations appear at  $1535 \text{ cm}^{-1}$  and  $784\text{--}853 \text{ cm}^{-1}$ , and those corresponding to  $\nu(\text{M-O})$  and  $\nu(\text{M-O})$  stretching occur at  $420\text{--}550 \text{ cm}^{-1}$ . The Table 2 presents the values of the two band frequencies of asymmetrical and symmetrical vibrations of carboxylate group for 4-hydroxybenzoates of Co(II) and Na(I). The difference in the values,  $\Delta\nu(\text{OCO})$ , between the frequencies  $\nu_{\text{as}}\text{OCO}$  and  $\nu_{\text{s}}\text{OCO}$  in the cobalt(II) complex is nearly similar ( $222 \text{ cm}^{-1}$ ) to the sodium salt ( $\Delta\nu = 232 \text{ cm}^{-1}$ ). According to the spectroscopic criteria<sup>32,33</sup> the carboxylate ions appear to be Co-OO-Co bridging chelation (Formula 2). The bands at *ca.*  $1560 \text{ cm}^{-1}$  and  $\sim 1385 \text{ cm}^{-1}$  overlapping with  $\nu_{\text{s}}\text{OCO}$  are due respectively to  $\nu(\text{N}=\text{O})$  ( $\nu_1$ ) and  $\nu_{\text{as}}(\text{NO}_2)$  ( $\nu_5$ ) of the coordinated nitrate. The  $\nu_{\text{s}}(\text{NO}_2)$  ( $\nu_2$ ) is detected at *ca.*  $1100 \text{ cm}^{-1}$ . These facts are characteristic of bidentate chelating nitrate.<sup>32,33</sup> The separation  $\Delta\nu = \nu_1 - \nu_5$  has been used as criterion of differentiation between mono and bidentate chelating nitrates, with  $\Delta\nu$  increasing as the coordination changes from mono to bidentate and/or bridging modes. The magnitude of this separation for this complex (Fig. 1) is indicative of a bidentate nitrate.<sup>32</sup> As expected for symmetric bidentate coordination, the separation of the  $\nu_{\text{as}}$  ( $1607 \text{ cm}^{-1}$ ) and  $\nu_{\text{s}}$  ( $1385 \text{ cm}^{-1}$ ) of the cobalt(II) complex ( $222 \text{ cm}^{-1}$ ) is much smaller than those observed for uni-dentate coordination.<sup>32</sup>

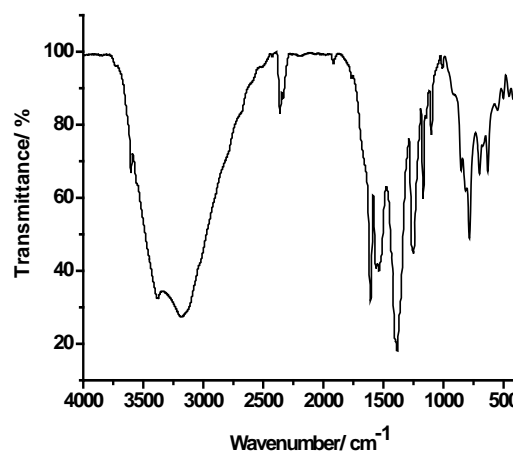


**Figure 1.** Infrared absorption spectrum of  $[\text{Co}_2(\text{C}_7\text{H}_5\text{O}_3)_2(\text{NO}_3)_2(\text{H}_2\text{O})_4] \cdot 2\text{H}_2\text{O}$  complex

### Electronic spectrum and magnetic measurements

The electronic UV-vis (Fig. 2), solid reflectance spectra and magnetic measurements are important and interesting items for most chemical characterizations to draw important information about the structural aspects of the transition metal complexes.<sup>34,35</sup> New bands in the visible region due to d-d absorption and charge transfer spectra from metal to ligand (M-L) or ligand to metal (L-M) can be observed and these data can be processed to obtain information regarding the structure and geometry of the complexes.<sup>34</sup> Electronic spectrum of cobalt(II) complex was recorded in DMSO with  $10^{-3} \text{ mol cm}^{-3}$ .

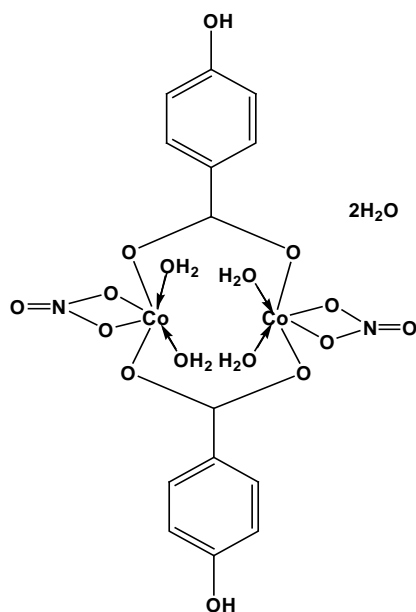
**Table 1:** Elemental analysis data of Co(II) p-hydroxybenzoate complex

Complex	C, %		H, %		N, %		Melting point, °C
	Calcd.	Found	Calcd.	Found	Calcd.	Found	
[Co <sub>2</sub> (C <sub>7</sub> H <sub>5</sub> O <sub>3</sub> ) <sub>2</sub> (NO <sub>3</sub> ) <sub>2</sub> (H <sub>2</sub> O) <sub>4</sub> ].2H <sub>2</sub> O	26.85	26.28	3.86	3.48	4.47	4.41	257

**Table 2:** Infrared frequencies (cm<sup>-1</sup>) and tentative assignments for Co(II) and Na(I) 4-hydroxybenzoate

Compounds	Assignments					
	V(O-H)	δ(H <sub>2</sub> O)	V <sub>as</sub> (OCO)	V <sub>s</sub> (OCO)	V <sub>as</sub> - V <sub>s</sub>	V(M-O)
[Co <sub>2</sub> (C <sub>7</sub> H <sub>5</sub> O <sub>3</sub> ) <sub>2</sub> (NO <sub>3</sub> ) <sub>2</sub> (H <sub>2</sub> O) <sub>4</sub> ].2H <sub>2</sub> O	3602	1607	1607	1385	222	550 501
	3381					453 420
Na(C <sub>7</sub> H <sub>5</sub> O <sub>3</sub> )	-	-	1610	1378	232	492

UV-visible peaks corresponding to the  $\pi \rightarrow \pi^*$  transitions in the Co(II) complex was observed at 274 and 294 nm for this complex, while the peaks belonging to  $n \rightarrow \pi^*$  transitions are recorded at 316 and 390 nm wavelengths. Also, remaining peaks at 536 and 584 cm<sup>-1</sup> can be attributed to the ligand-to-metal charge transfer bands LMCT.<sup>35</sup> In paramagnetic cobalt(II) complex, often the magnetic moment ( $\mu_{\text{eff}}$ ) gives the spin only value ( $\mu_{\text{s.o.}} = (n(n+2))^{1/2}$  B.M.) corresponding to the number of unpaired electron. The variation from the spin only value is attributed to the orbital contribution and it varies with the nature of coordination and consequent delocalization. The magnetic moment, configurations, stereochemistry, hybrid orbitals, number of unpaired electrons, spin-only and expected magnetic values of cobalt(II) p-hydroxybenzoate complex are (4.45 B.M., d<sup>7</sup>, octahedral, sp<sup>3</sup>d<sup>2</sup>, n=3, 3.88 B.M.). The diffuse spectrum for distorted octahedral of Co(II) complex, the diffuse spectrum displayed two bands at 16447 and 31746 cm<sup>-1</sup>, assigned to  $^4T_{1g}(F) \rightarrow ^4T_{2g}(F)$ , and  $^4T_{1g}(F) \rightarrow ^4A_{2g}(F)$  transitions, respectively.

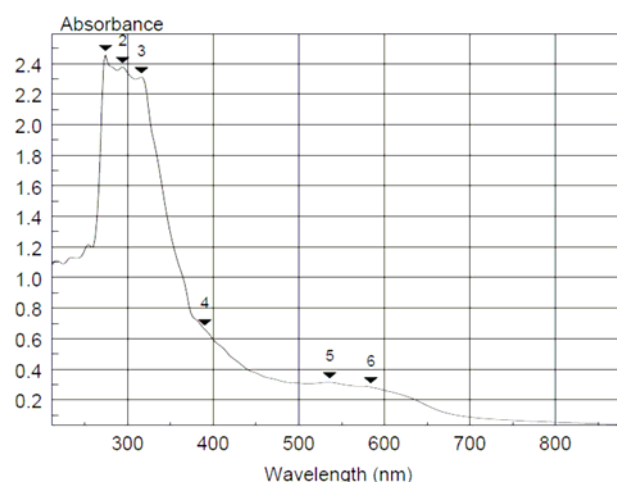
**Formula 2.** Suggested structure of the studied [Co<sub>2</sub>(C<sub>7</sub>H<sub>5</sub>O<sub>3</sub>)<sub>2</sub>(NO<sub>3</sub>)<sub>2</sub>(H<sub>2</sub>O)<sub>4</sub>].2H<sub>2</sub>O complex

### X-ray powder diffraction and scanning electron microscopy

There are fourteen peaks ( $2\theta/\text{intensity} = 5/100; 10/65; 14/23; 15/38; 18/21; 19/20; 21/25; 26/26; 27/39; 32/25; 34/19; 37/21; 43/25$  and  $47/19$ ) exhibited clearly in x-ray powder diffraction patterns (Fig. 3) of [Co<sub>2</sub>(C<sub>7</sub>H<sub>5</sub>O<sub>3</sub>)<sub>2</sub>(NO<sub>3</sub>)<sub>2</sub>(H<sub>2</sub>O)<sub>4</sub>].2H<sub>2</sub>O complex which was confirmed its crystalline structure. The values of  $2\theta$ ,  $d$  value (the volume average of the crystal dimension normal to diffracting plane), full width at half maximum (FWHM) of prominent intensity peak, relative intensity (%) and particle size of cobalt(II) 4-hydroxybenzoate complex was calculated. The maximum diffraction patterns of this complex exhibited at  $2\theta/d\text{-value}(\text{\AA}) = 5/1.2871$ . The crystallite size could be estimated from XRD patterns by applying FWHM of the characteristic peaks using Deby-Scherrer Eq. 1.<sup>36,37</sup>

$$D = K\lambda/\beta\cos\theta \dots \dots \dots (1)$$

where  $D$  is the particle size of the crystal grain,  $K$  is a constant (0.94 for Cu grid),  $\lambda$  is the X-ray wavelength (1.5406 Å),  $\theta$  is the Bragg diffraction angle and  $\beta$  is the integral peak width. The particle size was estimated according to the highest value of intensity compared with the other peaks. These data gave an impression that the particle size located within nano scale range.

**Figure 2.** Electronic spectrum of the studied [Co<sub>2</sub>(C<sub>7</sub>H<sub>5</sub>O<sub>3</sub>)<sub>2</sub>(NO<sub>3</sub>)<sub>2</sub>(H<sub>2</sub>O)<sub>4</sub>].2H<sub>2</sub>O complex

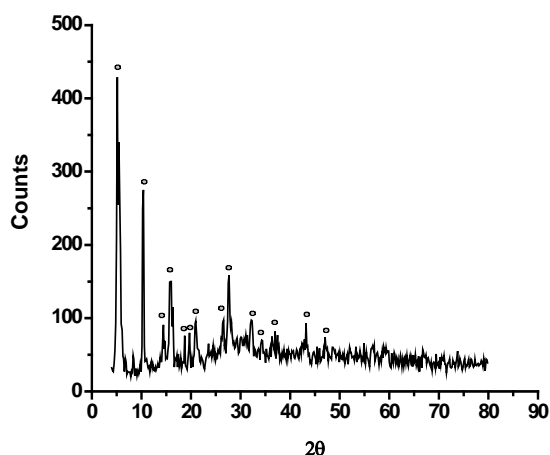


**Figure 3:** X-ray powder diffraction patterns of  $[\text{Co}_2(\text{C}_7\text{H}_5\text{O}_3)_2(\text{NO}_3)_2(\text{H}_2\text{O})_4]\cdot 2\text{H}_2\text{O}$  complex.

The morphology and particle size of  $[\text{Co}_2(\text{C}_7\text{H}_5\text{O}_3)_2(\text{NO}_3)_2(\text{H}_2\text{O})_4]\cdot 2\text{H}_2\text{O}$  complex has been discussed under using scanning electron microscopy (Fig. 4). This figure show the photographs at different magnitude 1000x, 2000x, 4000x, 5000x, 10 000x and 20 000x. From the collected photos, we can concluded that the cobalt(II) complex has a clear homogeneous phase with 4  $\mu\text{m}$  particle size.

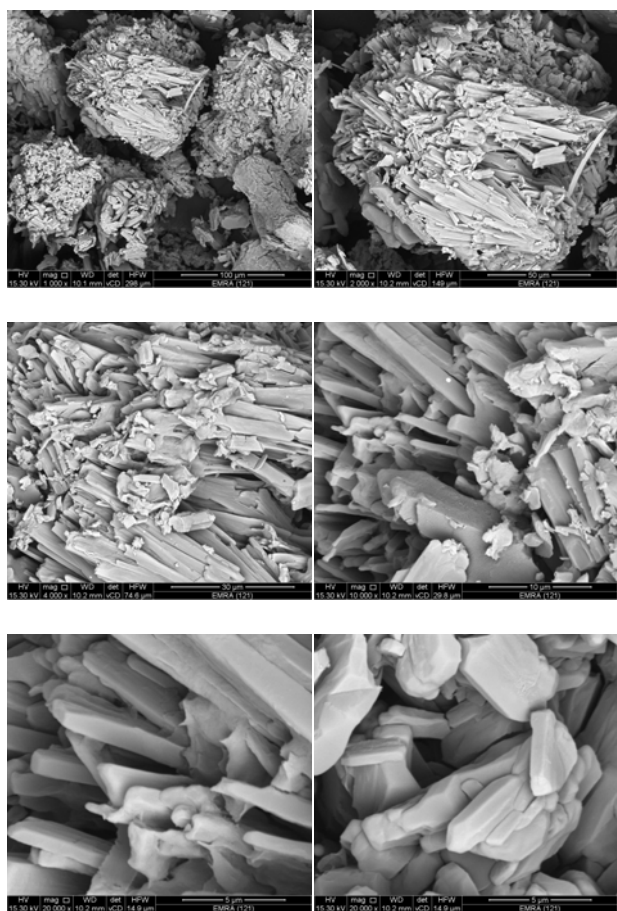


**Figure 4.** SEM photograph of the studied  $[\text{Co}_2(\text{C}_7\text{H}_5\text{O}_3)_2(\text{NO}_3)_2(\text{H}_2\text{O})_4]\cdot 2\text{H}_2\text{O}$  complex.

### Thermal and kinetic thermodynamic assessments

The data represented to the thermal decomposition of the synthetic cobalt(II) of 4-hydroxybenzoate,  $[\text{Co}_2(\text{C}_7\text{H}_5\text{O}_3)_2(\text{NO}_3)_2(\text{H}_2\text{O})_4]\cdot 2\text{H}_2\text{O}$ , complex are discussed as follows; The TG curve corresponding to this complex heated in the 30-800  $^{\circ}\text{C}$  temperature range is exhibited in Fig. 5. The thermal curve of cobalt(II) complex was recorded in static air atmosphere from ambient to 800  $^{\circ}\text{C}$ , the characteristic data and stages of pyrolysis regarding the thermal behavior refer that the resulted cobalt(II) complex is thermally stable up to 500  $^{\circ}\text{C}$ . The initiation of the mass loss in TG curve ascribed to dehydration of five water molecules with 14.05 % experimental value in agreement with calculated value 14.37 %. The second step in temperature range 176-310  $^{\circ}\text{C}$  at  $\text{DTG}_{\text{max}} = 257$   $^{\circ}\text{C}$  accompanied by losses of 2 nitrate and the last water molecules (calcd.=22.68 %; experimental = 22.06%). The third decomposition stage (decomposition of both 4-hydroxybenzoic acid moieties) appears as an endothermic peak 403  $^{\circ}\text{C}$  in the DTG curve. The residue left (calc.= 26.49%; experimental= 24.849%) in the crucible of corresponding cobalt(III) oxide  $\text{Co}_2\text{O}_3$  which is confirmed by infrared spectrum (Fig. 6).

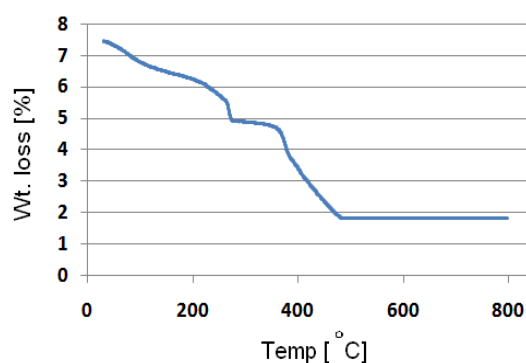


**Figure 5:** TG curve of  $[\text{Co}_2(\text{C}_7\text{H}_5\text{O}_3)_2(\text{NO}_3)_2(\text{H}_2\text{O})_4]\cdot 2\text{H}_2\text{O}$  complex

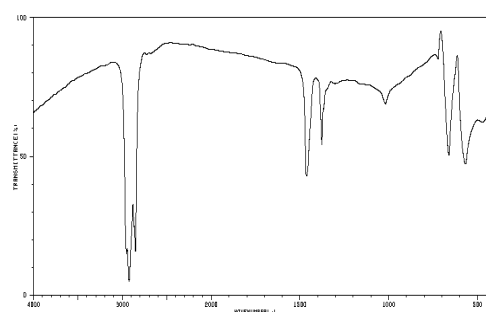


**Figure 6.** Infrared spectrum of final residue of  $[\text{Co}_2(\text{C}_7\text{H}_5\text{O}_3)_2(\text{NO}_3)_2(\text{H}_2\text{O})_4]\cdot 2\text{H}_2\text{O}$  complex at 800  $^{\circ}\text{C}$ .

In recent years there has been increasing interest in determining the rate-dependent parameters of solid-state non-isothermal decomposition reactions by analysis of TG curves. Several equations<sup>38-45</sup> have been proposed as means of analyzing a TG curve and obtaining values for kinetic parameters.

**Table 3:** Kinetic parameters determined using the Coats-Redfern (CR) and Horowitz-Metzger (HM).

Step	Horowitz-Metzger					Coats-Redfern				
	E, kJmol <sup>-1</sup>	Z, s <sup>-1</sup>	ΔS, J mol <sup>-1</sup> K <sup>-1</sup>	ΔH, kJ mol <sup>-1</sup>	ΔG, kJ mol <sup>-1</sup>	E, kJ mol <sup>-1</sup>	Z, s <sup>-1</sup>	ΔS, J mol <sup>-1</sup> K <sup>-1</sup>	ΔH, kJ mol <sup>-1</sup>	ΔG, kJ mol <sup>-1</sup>
2	97.4	4.12E+07	-104	93.0	148	87.1	3.28E+06	-125	82.7	149

Many authors<sup>38-42</sup> have discussed the advantages of this method over the conventional isothermal method. The rate of a decomposition process can be described as the product of two separate functions of temperature and conversion,<sup>39</sup> using

$$\frac{d\alpha}{dt} = k(T)f(\alpha) \quad (1)$$

where  $\alpha$  is the fraction decomposed at time  $t$ ,  $k(T)$  is the temperature dependent function and  $f(\alpha)$  is the conversion function dependent on the mechanism of decomposition. It has been established that the temperature dependent function  $k(T)$  is of the Arrhenius type and can be considered as the rate constant  $k$ .

$$k = Ae^{-\frac{E^*}{RT}} \quad (2)$$

where,  $R$  is the gas constant in (J mol<sup>-1</sup> K<sup>-1</sup>). Substituting Eqn. (2) into Eqn. (1), we get,

$$\frac{d\alpha}{dT} = \left[ \frac{A}{\phi} e^{-\frac{E^*}{RT}} \right] f(\alpha) \quad (3)$$

where,  $\phi$  is the linear heating rate  $dT/dt$ . On integration and approximation, this equation can be obtained in the following form:

$$\ln g(\alpha) = -\frac{E^*}{RT} + \ln \left[ \frac{AR}{\phi E^*} \right] \quad (4)$$

where  $g(\alpha)$  is a function of  $\alpha$  dependent on the mechanism of the reaction. The integral on the right hand side is assigned for temperature and has not so close for solution. So, several techniques have been used for the evaluation of temperature integral. Most commonly used methods for this purpose are the differential method of Freeman and Carroll<sup>38</sup> integral method of Coats and Redfern,<sup>40</sup> the approximation method of Horowitz and Metzger.<sup>43</sup> In the present investigation the general thermal behavior of the [Co<sub>2</sub>(C<sub>7</sub>H<sub>5</sub>O<sub>3</sub>)<sub>2</sub>(NO<sub>3</sub>)<sub>2</sub>(H<sub>2</sub>O)<sub>4</sub>].2H<sub>2</sub>O complex in terms of stability ranges, peak temperatures and values of kinetic parameters, are shown in Fig. 7 and Table 3. The kinetic parameters have been evaluated using the following methods and the results obtained by

these methods are compared with one another. The following two methods are discussed in brief.

#### Coats-Redfern equation

$$\int_0^\infty \frac{d\alpha}{(1-\alpha)^n} = \frac{A}{\phi} \int_{T_1}^{T_2} e^{-\frac{E^*}{RT}} dT \quad (5)$$

The Coats-Redfern equation, which is a typical integral method, can be represented as:

For convenience of integration the lower limit  $T_1$  is usually taken as zero. This equation on integration gives;

$$\ln \left[ -\frac{\ln(1-\alpha)}{T^2} \right] = -\frac{E^*}{RT} + \ln \left[ \frac{AR}{\phi E^*} \right] \quad (6)$$

A plot of left-hand side (LHS) against  $1/T$  was drawn.  $E^*$  is the energy of activation in kJ mol<sup>-1</sup> and calculated from the slope and  $A$  in (s<sup>-1</sup>) from the intercept value. The entropy of activation  $\Delta S^*$  in (J K<sup>-1</sup> mol<sup>-1</sup>) was calculated by using the equation:

$$\Delta S^* = R \ln \left[ \frac{Ah}{k_B T_s} \right] \quad (7)$$

where,  $k_B$  is the Boltzmann constant,  $h$  is the Planck's constant and  $T_s$  is the DTG peak temperature.<sup>46</sup>

#### Horowitz-Metzger equation

The Horowitz-Metzger equation is an illustrative of the approximation methods. These authors derived the relation:

$$\lg \left[ \frac{1-(1-\alpha)^{1-n}}{1-n} \right] = \frac{E^* \theta}{2.303RT_s^2} \quad \text{for } n \neq 1 \quad (8)$$

when  $n=1$ , the LHS of Eqn. 4 would be  $\lg[-\lg(1-\alpha)]$ . For

$$\lg \left[ \lg \frac{w_\alpha}{w\gamma} \right] = \frac{E\theta}{2.303RT_s^2} - \lg 2.303 \quad (9)$$

a first-order kinetic process the Horowitz-Metzger equation may be written in the form:

where  $\theta = T - T_s$ ,  $w_\gamma = w_\alpha - w$ ,  $w_\alpha$  = mass loss at the completion of the reaction;  $w$  = mass loss up to time  $t$ . The plot of  $\lg[\lg(w_\alpha/w_\gamma)]$  vs  $\theta$  was drawn and found to be linear from the slope of which  $E^*$  was calculated. The pre-exponential factor,  $A$ , was calculated from the equation:

$$\frac{E^*}{RT_s^2} = \frac{A}{\left[ \varphi \exp\left(-\frac{E^*}{RT_s}\right) \right]} \quad (10)$$

The entropy of activation,  $\Delta S^*$ , was calculated from Eqn. 3. The enthalpy activation,  $\Delta H^*$ , and Gibbs free energy,  $\Delta G^*$ , were calculated from:

$$\Delta H^* = E^* - RT \quad (11)$$

and

$$\Delta G^* = \Delta H^* - T\Delta S^* \quad (12)$$

respectively.

The activation energy  $E$ , increases through the degradation steps revealing the high stability of the remaining part suggesting a high stability of complexes characterization by covalence bonding. The negative of activation entropy values indicates that the activated fragment has more ordered structures. The positive of activation Gibbs's free energy reveals that the free energy of the final residue is higher than that of the initial complex and the decomposition stages are non spontaneous.

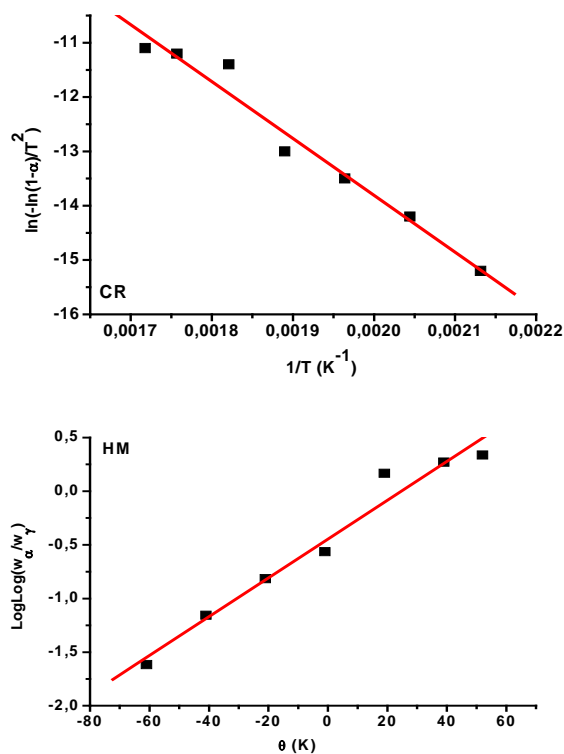


**Figure 7:** Plots of Coats-Redfern (CR) and Horowitz-Metzger (HM) relations for  $[\text{Co}_2(\text{C}_7\text{H}_5\text{O}_3)_2(\text{NO}_3)_2(\text{H}_2\text{O})_4] \cdot 2\text{H}_2\text{O}$  complex.

### Molecular modeling studies

Molecular modeling had been successfully used to detect three dimensional arrangements of atoms in free 4-hydroxybenzoic acid ligand and its cobalt(II) complex. The bond lengths and bond angles values of the chelation complex were summarized and recorded in Table 4 and Figs. 8a-b. This calculation for  $[\text{Co}_2(\text{C}_7\text{H}_5\text{O}_3)_2(\text{NO}_3)_2(\text{H}_2\text{O})_4] \cdot 2\text{H}_2\text{O}$  complex was obtained by using the commercial available molecular modeling software Chem Office Ultra-7. These statistical data have a good agreement with formula 2 confirmed the place of coordination towards cobalt(II) ions.

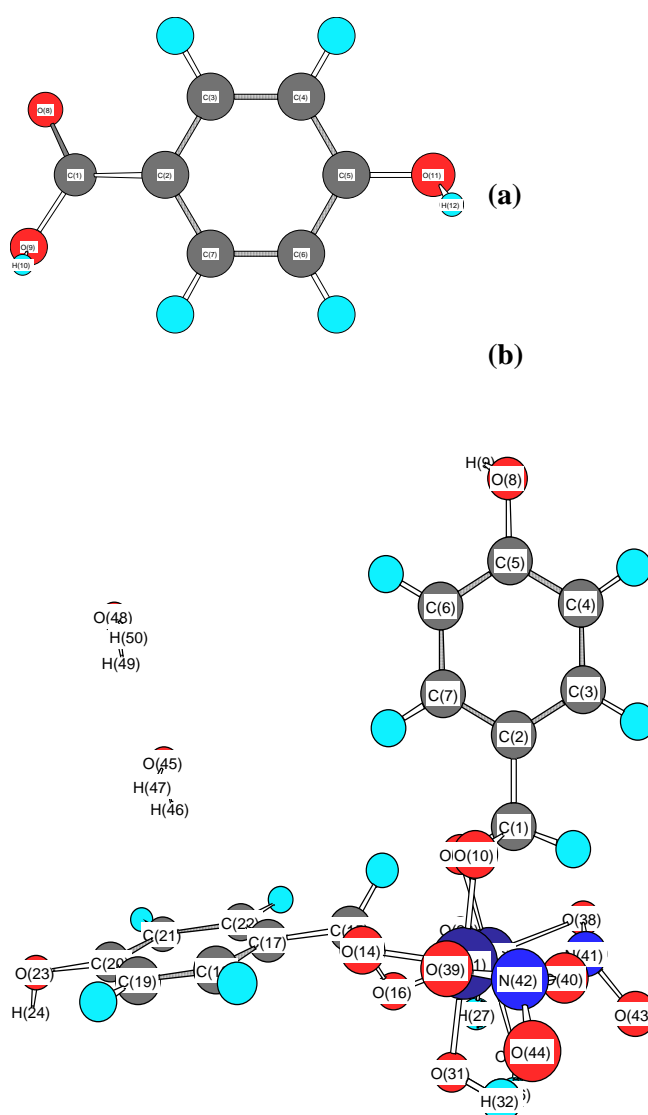


**Figure 8:** Molecular modeling of (a) 4-hydroxybenzoic acid and (b) its cobalt(II) complex

**Table 4:** The values of bond lengths and bond angles of 4-hydroxybenzoic acid and its cobalt complex

Adducts	Bond length			Bond angle		
	Atoms	Actual	Optimal	Atoms	Actual	Optimal
Ligand	C(1)-C(2)	1.517	1.517	C(2)-C(1)-O(8)	119.898	123
	C(1)-O(8)	1.208	1.208	C(2)-C(1)-O(9)	121.199	124.3
	C(1)-O(9)	1.338	1.338	O(8)-C(1)-O(9)	118.898	122
	C(2)-C(3)	1.42	1.42	C(1)-C(2)-C(3)	117.601	117.6
	C(2)-C(7)	1.42	1.42	C(1)-C(2)-C(7)	117.601	117.6
	C(3)-C(4)	1.42	1.42	C(3)-C(2)-C(7)	120	120
	C(3)-(16)	1.1	1.1	C(2)-C(3)-C(4)	120	120
	C(4)-C(5)	1.42	1.42	C(2)-C(3)-H(16)	119.998	120
	C(4)-(13)	1.1	1.1	C(4)-C(3)-H(16)	119.998	120
	C(5)-C(6)	1.42	1.42	C(3)-C(4)-C(5)	120	120
	C(5)-(11)	1.355	1.355	C(3)-C(4)-H(13)	119.998	120
	C(6)-C(7)	1.42	1.42	C(5)-C(4)-H(13)	119.998	120
	C(6)-(14)	1.1	1.1	C(4)-C(5)-C(6)	120.001	120
	C(7)-(15)	1.1	1.1	C(4)-C(5)-O(11)	119.998	124.3
	O(9)-(10)	0.972	0.972	C(6)-C(5)-O(11)	119.998	124.3
	O(11)-(12)	0.972	0.972	C(5)-C(6)-C(7)	120	120
				C(5)-C(6)-H(14)	119.998	120
				C(7)-C(6)-H(14)	119.998	120
				C(2)-C(7)-C(6)	120	120
				C(2)-C(7)-H(15)	119.998	120
			C(6)-C(7)-H(15)	119.998	120	
			C(1)-O(9)-H(10)	106.101	106.1	
			C(5)-O(11)-H(12)	108		
Co <sup>2+</sup>	C(1)-C(2)	1.497	1.497	C(2)-C(1)-O(10)	109.5	109.5
	C(1)-O(10)	1.402	1.402	C(2)-C(1)-O(13)	109.5	109.5
	C(1)-O(13)	1.402	1.402	C(2)-C(1)-H(60)	109.391	109.39
	C(1)-H(60)	1.109	1.109	O(10)-C(1)-O(13)	97.000	97
	C(2)-C(3)	1.42	1.42	O(10)-C(1)-H(60)	106.700	106.7
	C(2)-C(7)	1.42	1.42	O(13)-C(1)-H(60)	123.488	106.7
	C(3)-C(4)	1.42	1.42	C(1)-C(2)-C(3)	121.4	121.4
	C(3)-H(59)	1.1	1.1	C(1)-C(2)-C(7)	118.599	121.4
	C(4)-C(5)	1.42	1.42	C(3)-C(2)-C(7)	120	120
	C(4)-H(56)	1.1	1.1	C(2)-C(3)-C(4)	120	120
	C(5)-C(6)	1.42	1.42	C(2)-C(3)-H(59)	119.998	120
	C(5)-O(8)	1.355	1.355	C(4)-C(3)-H(59)	119.998	120
	C(6)-C(7)	1.42	1.42	C(3)-C(4)-C(5)	120.001	120
	C(6)-H(57)	1.1	1.1	C(3)-C(4)-H(56)	119.998	120
	C(7)-H(58)	1.1	1.1	C(5)-C(4)-H(56)	119.998	120
	O(8)-H(9)	0.972	0.972	C(4)-C(5)-C(6)	120.001	120
	O(10)-Co(11)	1.8		C(4)-C(5)-O(8)	119.998	124.3
	Co(11)-O(14)	1.8		C(6)-C(5)-O(8)	119.998	124.3
	Co(11)-O(25)	1.8		C(5)-C(6)-C(7)	120	120
	Co(11)-O(31)	1.8		C(5)-C(6)-H(57)	119.998	120
Co(11)-O(39)	1.8		C(7)-C(6)-H(57)	119.998	120	



Co(11)-O(40)	1.8		C(2)-C(7)-C(6)	120	120
Co(12)-O(13)	1.8		C(2)-C(7)-H(58)	119.998	120
Co(12)-O(16)	1.8		C(6)-C(7)-H(58)	119.998	120
Co(12)-O(28)	1.8		C(5)-O(8)-H(9)	108	108
Co(12)-O(34)	1.8		C(1)-O(10)-Co(11)	109.47	
Co(12)-O(37)	1.8		O(10)-Co(11)-O(14)	90	
Co(12)-O(38)	1.8		O(10)-Co(11)-O(25)	90	
O(14)-C(15)	1.402	1.402	O(10)-Co(11)-O(31)	180	
C(15)-O(16)	1.402	1.402	O(10)-Co(11)-O(39)	89.999	
C(15)-C(17)	1.497	1.497	O(10)-Co(11)-O(40)	89.999	
C(15)-H(55)	1.109	1.109	O(14)-Co(11)-O(25)	90	
C(17)-C(18)	1.42	1.42	O(14)-Co(11)-O(31)	90	
C(17)-C(22)	1.42	1.42	O(14)-Co(11)-O(39)	90	
C(18)-C(19)	1.42	1.42	O(14)-Co(11)-O(40)	180	
C(18)-H(54)	1.1	1.1	O(25)-Co(11)-O(31)	89.999	
C(19)-C(20)	1.42	1.42	O(25)-Co(11)-O(39)	180	
C(19)-H(52)	1.1	1.1	O(25)-Co(11)-O(40)	89.999	
C(20)-C(21)	1.42	1.42	O(31)-Co(11)-O(39)	90	
C(20)-O(23)	1.355	1.355	O(31)-Co(11)-O(40)	90	
C(21)-C(22)	1.42	1.42	O(39)-Co(11)-O(40)	90	
C(21)-H(51)	1.1	1.1	O(13)-Co(12)-O(16)	89.658	
C(22)-H(53)	1.1	1.1	O(13)-Co(12)-O(28)	90	
O(23)-H(24)	0.972	0.972	O(13)-Co(12)-O(34)	180	
O(25)-H(26)	0.992		O(13)-Co(12)-O(37)	90	
O(25)-H(27)	0.992		O(13)-Co(12)-O(38)	90	
O(28)-H(29)	0.992		O(16)-Co(12)-O(28)	90	
O(28)-H(30)	0.992		O(16)-Co(12)-O(34)	90.341	
O(31)-H(32)	0.992		O(16)-Co(12)-O(37)	90	
O(31)-H(33)	0.992		O(16)-Co(12)-O(38)	179.684	
O(34)-H(35)	0.992		O(28)-Co(12)-O(34)	90	
O(34)-H(36)	0.992		O(28)-Co(12)-O(37)	180	
O(37)-N(41)	1.316		O(28)-Co(12)-O(38)	90	
O(38)-N(41)	1.864		O(34)-Co(12)-O(37)	90	
O(39)-N(42)	1.316		O(34)-Co(12)-O(38)	90	
O(40)-N(42)	1.864		O(37)-Co(12)-O(38)	90	
N(41)-O(43)	1.316		C(1)-O(13)-Co(12)	109.472	
N(42)-O(44)	1.316		Co(11)-O(14)-C(15)	109.47	
O(45)-H(46)	0.942	0.942	O(14)-C(15)-O(16)	97	97
O(45)-H(47)	0.942	0.942	O(14)-C(15)-C(17)	109.5	109.5
O(48)-H(49)	0.942	0.942	O(14)-C(15)-H(55)	106.7	106.7
O(48)-H(50)	0.942	0.942	O(16)-C(15)-C(17)	109.5	109.5
			O(16)-C(15)-H(55)	106.7	106.7
			C(17)-C(15)-H(55)	124.049	109.39
			Co(12)-O(16)-C(15)	109.262	
			C(15)-C(17)-C(18)	120	121.4
			C(15)-C(17)-C(22)	119.998	121.4
			C(18)-C(17)-C(22)	119.998	120
			C(17)-C(18)-C(19)	120	120

C(17)-C(18)-H(54)	119.998	120
C(19)-C(18)-H(54)	120	120
C(18)-C(19)-C(20)	119.998	120
C(18)-C(19)-H(52)	119.998	120
C(20)-C(19)-H(52)	119.998	120
C(19)-C(20)-C(21)	120	120
C(19)-C(20)-O(23)	119.998	124.3
C(21)-C(20)-O(23)	119.998	124.3
C(20)-C(21)-C(22)	120.001	120
C(20)-C(21)-H(51)	119.998	120
C(22)-C(21)-H(51)	119.998	120
C(17)-C(22)-C(21)	120	120
C(17)-C(22)-H(53)	119.998	120
C(21)-C(22)-H(53)	119.998	120
C(20)-O(23)-H(24)	108	108
Co(11)-O(25)-H(26)	109.482	
Co(11)-O(25)-H(27)	109.461	
H(26)-O(25)-H(27)	0.316	
Co(12)-O(28)-H(29)	109.451	
Co(12)-O(28)-H(30)	109.468	
H(29)-O(28)-H(30)	0.547	
Co(11)-O(31)-H(32)	109.535	
Co(11)-O(31)-H(33)	109.468	
H(32)-O(31)-H(33)	0.547	
Co(12)-O(34)-H(35)	109.451	
Co(12)-O(34)-H(36)	109.444	
H(35)-O(34)-H(36)	0.547	
Co(12)-O(37)-N(41)	90	
Co(12)-O(38)-N(41)	74.951	
Co(11)-O(39)-N(42)	90	
Co(11)-O(40)-N(42)	74.951	
O(37)-N(41)-O(38)	105.05	
O(37)-N(41)-O(43)	109.47	
O(38)-N(41)-O(43)	109.47	
O(39)-N(42)-O(40)	105.05	
O(39)-N(42)-O(44)	109.47	
O(40)-N(42)-O(44)	109.47	
H(46)-O(45)-H(47)	103.7	103.7
H(49)-O(48)-H(50)	103.702	103.7

### Biological activity studies

The biological assessment were studied in term of antimicrobial activities of  $[\text{Co}_2(\text{C}_7\text{H}_5\text{O}_3)_2(\text{NO}_3)_2(\text{H}_2\text{O})_4]2\text{H}_2\text{O}$  complex against gram-positive (*Bacillus subtilis* and *Staphylococcus aureus*) and gram-negative (*Escherichia coli* and

*Pseudomonas aeruginosa*) and two strains of fungi (*Aspergillus flavus* and *Candida albicans*). Results from the agar disc diffusion tests for antimicrobial activities of respective complex are shown in Fig. 9. The tested cobalt(II) complex displayed a different degree of antimicrobial effect (*Staphylococcus aureus* > *Bacillus subtilis* = *Escherichia coli* = *Candida albicans* > *Pseudomonas aeruginosa* > *Aspergillus flavus*) and has a

degree of antimicrobial activities greater than free ligand against all organisms tested. The various reasons for lethal action of tested complex may be due to their interactions with critical intra-cellular sites causing the death of cells. The variety of antimicrobial activities of tested complex may be due to a penetration through cell membrane structure of target organism. In conclusion, the interaction between the tested cobalt(II) complex in nano-structural form resulting in developing the effectiveness of biological characters of free p-hydroxybenzoic acid.

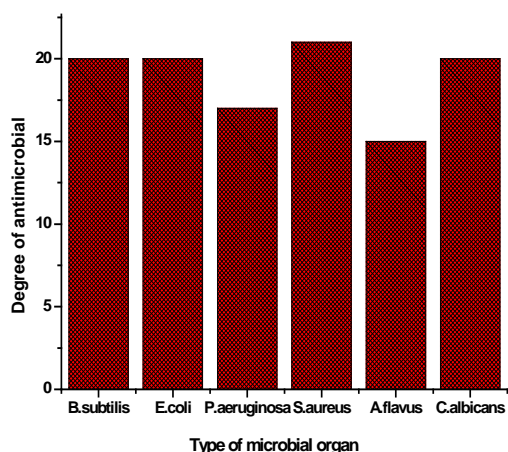


Figure 9. Biological assessment of cobalt(II) complex.

## Conclusion

The interaction between the 4-hydroxybenzoic acid and the cobalt nitrate hydrated synthesized using microwave technique and was studied spectroscopically. New cobalt(II) complex was isolated and characterized through elemental analysis, (infrared, electronic, SEM and XRD spectra) and also thermal and kinetic thermodynamic studies. The stoichiometry of the product was found to be 1:1. Accordingly, the formed CT-complex has the formula  $[\text{Co}_2(\text{C}_7\text{H}_5\text{O}_3)_2(\text{NO}_3)_2(\text{H}_2\text{O})_4] \cdot 2\text{H}_2\text{O}$ .

## Acknowledgement

This work was supported by grants from Taif University, Taif, Saudi Arabia under project Grants No. 1242-432-1.

## References

- Dey, G. Chakraborty, M., Mitra, A. *J. Plant Physiology*, **2005**, 162(4), 375.
- Pietta, P. G. Simonetti, P. Gardana, C. Brusamolino, A. Morazzoni, P. Bombardelli, E. *BioFactors*, **1998**, 8(1-2), 111.
- Wiegardt, K. *Angew. Chem. Int. Ed. (Engl.)*, **1989**, 28, 1153.
- Pecoraro, V. L. Baldwin, M. S. Gelasco, A., *Chem. Rev.*, **1994**, 94, 807.
- Rane, K. S. Verenkar, V. M. S., *Bull. Mater. Sci.*, **2001**, 24, 39.
- Lambi, J.N. Nsehyuka, A.T. Egbeatt, N. Cafferata, L.F.R. Arvia, A.J. *Thermochim. Acta*, **2003**, 398, 145.
- Mehrotra, R. C. Singh, A. *Progr. Chem.*, **1997**, 46, 239.
- Srinivasan, B. R. Sawant, S. C. *Thermochim. Acta*, **2003**, 402 45.
- Wells, M. A. Bruce, T. C., *J. Am. Chem. Soc.*, **1977**, 99, 5341.
- Breslow, R. McClure, D. E. Brown, R.S. Eisenach, J., *J. Am. Chem. Soc.*, **1975**, 97, 194.
- Kato, C.N. Mori, W., *Comp. Rend. Chim.*, **2007**, 10(4), 284.
- Volkman, J. Nicholas, K. M. *Tetrahedron*, **2012**, 68(16), 3368.
- Reger, D. L. Debreczeni, A. Smith, M. D. *Inorg. Chim. Acta*, **2012**, 386, 102.
- Chen, Y. Liu, C. B. Gong, Y. N. Zhong, J. M. Wen, H. L. *Polyhedron*, **2012**, 36(1), 6.
- Mehrotra, R. C. Bohra, R., *Metal Carboxylates*, Academic Press, London, **1983**.
- Brusau, E. V. Pedregosa, J. C, Narda, G. E. Ayala, E. P. Oliveira, E. A., *J. Arg. Chem. Soc.*, **2004**, 92(1/3), 43.
- Deacon, G. B. Phillips, R. J. *Coord. Chem. Rev.*, **1980**, 33, 227.
- Alcock, N. W. Culver, J. Roe, S. M., *J. Chem. Soc. Dalton Trans.*, **1992**, 1447.
- Mahajan, K., Fahmi, N., Singh, R. V., *Indian J. Chem.*, **2007**, 46A, 1221.
- Mahajan, K. Swami, M. Singh, R. V. *Russ. J. Coord. Chem.*, **2009**, 35, 179.
- Mohanani, K. Kumari, S. Rijulal, G., *J. Rare Earths*, **2008**, 26, 16.
- Garg, R. Saini, M. K. Fahmi, N. Singh, R. V., *Trans. Met. Chem.*, **2006**, 31, 362.
- Sharma, K. Singh, R. Fahmi, N. Singh, R. V. *Spectrochim. Acta*, **2010**, 75A, 422.
- Bauer, A. W. Kirby, W. M. Sherris, C. Turck, M. *Amer. J. Clinical Pathology*, **1966**, 45, 493.
- Pfaller, M. A. Burmeister, L. Bartlett, M. A. Rinaldi, M. G. *J. Clin. Microbiol.* **1988**, 26, 1437.
- National Committee for Clinical Laboratory Standards, *Performance Vol. Antimicrobial susceptibility of Flavobacteria*, **1997**.
- National Committee for Clinical Laboratory Standards. **1993**. Methods for dilution antimicrobial susceptibility tests for bacteria that grow aerobically. Approved standard M7-A3. National Committee for Clinical Laboratory Standards, Villanova, Pa.
- National Committee for Clinical Laboratory Standards. **2002**. Reference Method for Broth Dilution Antifungal Susceptibility Testing of Conidium-Forming Filamentous Fungi: Proposed Standard M38-A. NCCLS, Wayne, PA, USA.
- National Committee for Clinical Laboratory Standards. **2003**. Methods for Antifungal Disk Diffusion Susceptibility Testing of Yeast: Proposed Guideline M44-P. NCCLS, Wayne, PA, USA.
- Liebowitz, L. D. Ashbee, H. R. Evans, E. G. V. Chong, Y. Mallatova, N. Zaidi, M. Gibbs, D. and Global Antifungal Surveillance Group., *Diagn. Microbiol. Infect.* **2001**. Dis. 4, 27.
- Matar, M. J. Ostrosky-Zeichner, L. Paetznick, V. L. Rodriguez, J. R. Chen, E. Rex, J. H. *Antimicrob. Agents Chemother.*, **2003**, 47, 1647.
- Nakamoto, K. *Infrared and Raman Spectra of Inorganic and Coordination Compounds*, John-Wiley and Sons, New York, **1997**.

- <sup>33</sup>Burger, K. *Coordination Chemistry: Experimental Methods*, Akademiai Kiadó, Budapest, **1973**.
- <sup>34</sup>Singh, H.L. Vershney, A.K. *Bioinorg. Chem. Appl.*, **2006**, 1.
- <sup>35</sup>Allan, J. R., Baird, N. D., Kassyk, A. L., *J. Therm. Anal.*, **1979**, 16, 79.
- <sup>36</sup>Cullity, B. D. Stock, S. R. *Elements of X-Ray Diffraction*, 3rd Ed., Prentice-Hall Inc., **2001**, p 167-171.
- <sup>37</sup>Jenkins R. and Snyder, R. L. *Introduction to X-ray Powder Diffractometry*, John Wiley & Sons Inc., **1996**, p 89-91.
- <sup>38</sup>Freeman, E.S. Carroll, B., *J. Phys. Chem.*, **1958**, 62, 394.
- <sup>39</sup>Sestak, J. Satava, V. Wendlandt, W.W., *Thermochim. Acta*, **1973**, 7, 333.
- <sup>40</sup>Coats, A. W., Redfern, J. P., *Nature*, **1964**, 201, 68.
- <sup>41</sup>Ozawa, T., *Bull. Chem. Soc. Jpn.*, **1965**, 38, 1881.
- <sup>42</sup>Wendlandt, W. W. *Thermal Methods of Analysis*, Wiley, New York, **1974**.
- <sup>43</sup>Horowitz, H. W. Metzger, G., *Anal. Chem.*, **1963**, 35, 1464.
- <sup>44</sup>Flynn, J. H. Wall, L. A., *Polym. Lett.*, **1966**, 4, 323.
- <sup>45</sup>Kofstad, P. *Nature*, **1957**, 179, 1362.
- <sup>46</sup>Flynn, J. H. F. Wall, L. A. *J. Res. Natl. Bur. Stand.*, **1996**, 70A, 487.

Received: 08.10.2012.

Accepted: 16.10.2012.